Estimation of Muscle Fiber Orientation in Ultrasound Images using Revoting Hough Transform (RVHT)

Yongjin Zhou and Yong-Ping Zheng

Department of Health Technology and Informatics,

The Hong Kong Polytechnic University, Hong Kong

Running Title: **Hough Transform for Muscle Ultrasound Images**

Corresponding author:

Yongping Zheng, PhD.

Department of Health Technology and Informatics,

The Hong Kong Polytechnic University,

Hung Hom, Kowloon, Hong Kong SAR, P.R.China

Tel: 852-27667664

Fax: 852-23624365

Email: ypzheng@ieee.org

Submitted to: Ultrasound in Medicine and Biology

First Submission: Oct 12, 2007

First Revision: Nov 7, 2007

Abstract

Ultrasound imaging has been frequently used for the study of muscle contraction, including measurements of pennation angles and fascicle orientations. However, these measurements were traditionally conducted by manually drawing lines on the ultrasound images. In this study, we proposed a modified Hough transform (HT), aiming at automatically estimating orientations of straight-line-shaped patterns, such as muscle fibers and muscle-bone interface in ultrasound images. The new method first located the global maximum in the HT accumulator matrix, which corresponded to the most dominant collinear feature points globally, using the standard HT; then the pixels close to the detected line were removed from the edge map, the HT accumulator matrix was calculated again, i.e. revoting, and a new line was detected; the iteration was repeated until the predefined termination conditions were satisfied. The performance of the algorithm was tested using computer-generated images with different levels of noises as well as clinical ultrasound images and compared with that of the conventional method. It was found that the orientation estimation results obtained by the new algorithm were well correlated (R^2 = 0.9902) with those obtained using the traditional method, i.e., drawing lines manually and reading the angles with the assistance of software. Further mean-difference plots revealed a difference of 0.18±2.41 degree between the two methods at the 95% confidence level. In comparison with the traditional method, the new algorithm was more capable of handling with highly noisy data, and could avoid the aliasing problem, i.e., reporting multiple lines instead of single expected line. The results of this study suggested that

the proposed revoting Hough transform can be potentially used for the reliable and non-subjective automatic estimation of the orientations of muscle fibers in musculoskeletal ultrasound images.

Keywords: Ultrasound, Muscle, Hough transform, Sonomyography

Introduction

Ultrasound imaging has been widely used to assess human muscles in both static and dynamic conditions. In recent years, it has been employed to measure the quantitative changes in muscle thickness (Misuri et al. 1997, Hodges et al. 2003), fiber pennation angle (Narici et al. 1996, Fukunaga et al. 1997, Ito et al. 1998, Maganaris et al. 2002), fascicle length (Misuri et al. 1997, Narici et al. 1996, Fukunaga et al. 1997, Ito et al. 1998, Maganaris et al. 2002, Mademli and Arampatzis 2005), and cross-sectional area (Narici et al. 1996, Reeves et al. 2004, Maganaris et al. 2006) during isometric and dynamic contractions. Since these architectural parameters change obviously with contraction, they could potentially provide a noninvasive method of recording activities of various muscles. During the measurement of muscle fiber length and pennation angle as well as fascicle length, the detection of line structures is frequently involved. Traditionally, the lines and angles in musculoskeletal ultrasound images used to be detected manually, or interactively using software (Reeves et al. 1994, Itoii et al. 2001), such as NIH Image (National Institutes of Health, Bethesda, MD, USA, http://rsb.info.nih.gov/nih-image). Using the software, the orientation of a manually drawn line on the studied image could be read. These methods were very time-consuming and the manual detecting process was subjective. Recently, we proposed the concept of sonomyography, which represents the signals about continuous changes of muscle thickness and pennation angle, which are detected from ultrasound images (Zheng et al. 2006, Shi et al. 2007a, 2007b, Guo et al. 2007). The manual detection of the orientation of muscle fiber and fascicle greatly hindered the real-time detection of muscle pennation angle for sonomyography. A real-time automatic orientation/angle estimation method for musculoskeletal ultrasound images is much desired for the further development and application of sonomyography techniques.

The detection of a straight line in an image is a fundamental problem in computer vision. The Hough transform (HT) (Hough et al. 1962) of slope-intercept parameterization as well as its improved version, HT of angle-radius parameterization (Duda and Hart 1972, Immerkar 1998), has been an established solution to the problem. As a major extension of HT, the generalized Hough transform (Ballard 1981) managed to detect more complex shapes, such as circles. While the probabilistic Hough transform (Kiryati et al. 1991) only used a small number of edge/feature points, selected from the original edge map, so as to significantly save computational time, at the cost of slightly impaired detection performance. For the standard Hough transform (SHT), many attentions have been paid to the aliasing problem, caused by the discrete nature of digital image and the discretization errors of HT (Kiryati and Bruckstein 1991, Van Veen and Groen 1981), Brown 1983, Kiryati et al. 1991, Yuen and Ma 1997, Lam et al. 1994). Using image-splitting and grouping, Princen et al (1990) proposed a hierarchical approach to achieve a robust architecturally important solution to several problems associated with SHT line detection, including the aliasing problem. For large-sized images such as engineering drawings, Song and Lyu (2005) recently reported a more comprehensive solution, utilizing both Hough space and image space information. However, it is difficult to directly use these methods for the images with high noise levels, such as ultrasound images with significant speckle noises.

In this study, we presented an improved HT method to identify the major muscle fascicles orientations in musculoskeletal ultrasound images, which may contain significant speckle noises. We proposed a revoting strategy to deal with the aliasing problem in the line detection for ultrasound images. A thresholding method using the data in HT space was proposed to control the detection of significant lines in the ultrasound image. We tested the performance of this new algorithm using computer-generated images with different levels of speckle noises and clinical musculoskeletal ultrasound images.

Methods

Standard Hough transform of angle-radius parameterization

SHT uses the normal parameterization of a straight line in an image (Duda and Hart

1972),

$$x\cos\theta_1 + y\sin\theta_1 = \rho_1 \quad (1)$$

where θ_1 is the angle between the normal of the line and the x-axis, ρ_1 is the distance of the coordinates origin to the line. The parameters of all straight lines going through a point (x_i, y_i) in the image space show up in the (ρ,θ) parameter space as a sinusoidal curve, given by

$$x_i\cos\theta + y_i\sin\theta = \rho \quad (2)$$

After transforming all edge/feature points to the (ρ,θ) space, the collinear points will cross each other and an array measuring the crossing situation is accumulated. Traditionally this array $H(\rho,\theta)$ is called accumulator array. The next stage of the SHT is an exhaustive search for the maxima in the accumulator array, and a predefined threshold is set so that all local values of $H(\rho,\theta)$ exceeding the threshold can be recognized as the evidence of straight lines existing in the original image space.

In summary, in SHT, the collinear edge/feature points in the image space show up as peaks in the (ρ,θ) space. However, in the realization of SHT, there arise some issues: 1) digital image is by nature discrete, 2) when mapped into (ρ,θ) space, θ also has to be sampled in a limited resolution and ρ has to be quantized, 3) $H(\rho,\theta)$ is also represented on a discrete grid where only integer coordinates have values, 4) The original image can suffer from various noises. These issues could cause problems of aliasing, peak spreading or peak extension (Kiryati and Bruckstein 1991, Van Veen and Groen 1981), Brown 1983, Kiryati et al. 1991, Yuen and Ma 1997, Lam et al. 1994).

Revoting Hough transform (RVHT)

To test the feasibility of using HT methods for the line orientation detection in musculoskeletal sonograms which are usually degraded by speckle noises, a modified Hough transform named as revoting Hough transform (RVHT) was adopted in this paper. The global maximum in the accumulator array, voted by all the edge/feature points, was first detected. Then all the feature points close to this line were removed from the edge map. With the updated edge map, the new accumulator array was computed and used to detect the global maximum by voting again. More lines could be identified by repeating this revoting procedure, as shown in Fig. 1. When the image was very noisy, the removal width could be extended from the basic value, 1 pixel, to several pixels (6-12 pixels were selected for the musculoskeletal ultrasound images with resolutions of 10 pixels/*mm* to 12.5 pixels/*mm* in this study) to remove more neighboring feature points along the location of the detected line. The center of the image was used as the origin of the coordinate system in HT, as suggested by Immerkar (1998).

Experiments and Results

Comparison of SHT and RVHT using a computer-generated image

A testing image (256x256), as shown in Fig. 2(a), was generated using Matlab 6.5.

The distances from the vertexes of the larger equilateral triangle (with a side length of 200 pixels) to the left, right and up borders of the image are all 28 pixels, while the distances from the vertexes of the smaller equilateral triangle (with a side length of 100 pixels) to the borders of the image are all 78 pixels. The base sides of both triangles are in horizontal direction. The gray level between the two equilateral triangles was uniformly set to 64 and the background gray level was 0. Next, a new image (Fig. 2(b)), was created by adding a Gaussian noise with a mean of 64 (gray level) and a standard deviation of 16 to the original image. The edge map of Fig. 2(b), acquired using the Sobel edge detector (Gonzalez and Woods 1992), is shown in Fig. 2(c). Using all edge pixels in Fig. 2(c), the accumulator array was then generated as shown in Fig.2(d), where the *x-axis* stands for θ (ranging from 0 to 360) and *y-axis* for ρ (ranging from 0 to the image diagonal length, 362 in this image), the labels for hereinafter accumulator arrays had same setting and therefore were omitted. Since in this implementation, the 'angle' is defined as the angle between the detected line and the vector pointing from the image up-left corner to the bottom-left corner, therefore for one single straight line, two angles were detected, i.e., θ and its inverted version along the same straight line, θ+180. Subsequently, the 12 brightness peaks in Fig. 2(d) corresponded to the 6 vertices of the 2 triangles, respectively. The specific correspondences would be further illustrated later when they were removed one by one from the most-voted one. For the purpose of a better display, the accumulator array brightness was rescaled in each iteration, i.e., the current most voted points were also displayed as 22 gray levels, therefore, Fig.2(i) seems to have more sinusoidal curves than Fig.2(d), but it's not the case. It's only because of the rescaling of the displayed gray range after pixel removal was changed. The resolution of $H(\rho,\theta)$ is 1 degree in x-axis and 1 pixel in y-axis, which could satisfy the Yuen's quantization schemes (Yuen and Ma 1997). When the SHT threshold was set to be 70% of the global maximum in $H(\rho,\theta)$, only the larger triangle was detected, as indicated in Fig. 2(e). And when the threshold was decreased to 50% of the global maximum to make the Hough voting procedure more sensitive, two sides of the inner triangle could be detected (Fig. 2(f)). However, in this case, some extra lines were also detected while the bottom side of the inner triangle was undetected, even though it is obvious in the image. The main reason was that some lines generated large values, i.e. bright region, in the accumulated array image. The maximum value was larger than double of the value generated by the bottom side of the inner triangle. To test a more noisy case, a Gaussian white noise with a mean of 64 and a standard deviation of 32 was added to Fig. 2(a), producing a new image of Fig. 2(g). Following above procedures, the corresponding new edge map and accumulator array were obtained (Fig. 2(h) and (i)). Fig. 2(j), (k) and (l) shows the new detection results acquired using threshold values of 70%, 50% and 40% of the global maximum in $H(\rho,\theta)$ respectively. Under this noise condition, the right side of the smaller triangle could not be detected with a 50% threshold. In addition, some extra lines could be observed, such as those near the base side of the larger triangle. When the threshold was further decreased to 40% of the global maximum in $H(\rho,\theta)$, more extra lines were detected.

As a comparison, the results of applying our RVHT to the image of Fig. 2(g) are presented in Fig. 3. Fig. 3(a) shows the obtained accumulator array, where the marked locations correspond to the two directions of the same straight line. The detected angle, defined as the angle between the detected line and the vector pointing from the image up-left corner to the bottom-left corner as in the software of NIH Image (Reeves et al. 1994), is 150/330^{o}, which is correct according to the value used for the image generation. Figure 3(b) shows the 'original image' (Fig. 2(g)) overlapped by the detected line and Fig. 3(c) the updated edge map where the edge/feature points corresponding to the detected line had been removed, with a removal width of 2 pixels. Similarly, using the RVHT, 30/210^{o} and 90/270^{o} directions of the larger triangle, and 90/270^{o}, 150/330^{o} and 30/210^{o} of the smaller triangle were detected and shown in the subsequent rows in Fig. 3 in turn.

Application of RVHT on musculoskeletal ultrasound images

From three healthy adult male volunteers, 45 ultrasound images on biceps and forearm muscles were acquired by an ultrasound image system (ATL HDI 5000, Philips Inc, Bothell, WA), and cropped to remove the imaging tags and retain the image content only. The human subject ethical approval was obtained from the relevant committee in the authors' institution and informed consents were obtained from subjects prior to the experiment. Totally 168 lines were detected using RVHT, among which 165 were regarded as being valid according to visual verification. A typical image and the corresponding products using RVHT are shown in Fig. 4, where (a) is the original image, (b) its Sobel edge map, (c) the HT accumulator array of (b), and (f) the detected lines after RVHT. The line detection results using SHT with thresholds of 80% and 60% were demonstrated in Fig. 4(d) and (e), respectively. Considering the complicated speckle noise conditions in the ultrasound images, the peaks in the corresponding HT accumulator array image were no longer as ‘sharp’ as those of the simulated image, as shown in Fig. 4(c). In such case, the removal width for RVHT could be set to 12 pixels and the angles detected were marked in the figure in the order they got detected.

At the same locations where lines were detected using RVHT, two operators manually drew lines on the original images and read the drawn angles using software (NIH Image). The angles estimated by the RVHT, operator #1 and operator #2 were defined as *ap*, *aa*1 and *aa*2, respectively. To investigate how well the RVHT results fitted the manually drawn values, we compared the RVHT result *ap* with the mean value of the two operators (*aa*1 + *aa*2) / 2. As shown in Fig. 5, a very good linear correlation between the results of the two methods was obtained ($R^2 = 0.9902$). Further mean – difference plots (Bland and Altman 1986) for the results as illustrated in Fig. 6 showed that the difference between *ap* and (*aa*1 + *aa*2) / 2 was 0.18±2.41 degree for the 95% confidence level.

The ratio of the feature points, counted by the number of pixels in the edge map, of the last and first detected lines could be controlled by the users. In this study, we used a ratio of 25%, and 5 lines could be normally detected in each image. A smaller ratio would cause more lines to be detected. This ratio together with the number of lines to be detected could be used as iteration termination conditions.

Discussions

From the results obtained in the current experiments, it was observed that the proposed RVHT had some advantages for the line/angle detection in the noisy images. Compared to SHT, the RVHT was inherently anti-aliasing as the feature points which had voted for a line were removed when the line was detected. As stated earlier, once the favored candidate line won the global voting, voices of these feature points were ignored in the subsequent voting, and so were those in the nearby neighborhoods (depending on the removal width). In case the image was very noisy, such as in many ultrasound images, the manual detection became more subjective and difficult. As demonstrated in this study, the proposed RVHT method could detect the lines with a performance comparable to that of manual operation. Moreover, the RVHT was almost automatic and could potentially save lots of manual work in comparison with the traditional way of orientation estimation in musculoskeletal ultrasound images. Therefore, the proposed RVHT has great potential for future image-guided US musculoskeletal analysis, especially for the automatic estimation of the muscle thickness and fascicle length. Furthermore, this new method was inherently objective, and when the US images to be processed are massive, the proposed method could be more advantageous than the manual method.

In spite of the above advantages, the proposed RVHT could be improved in a number of aspects. Similar to the selection of the threshold value in SHT, RVHT faces a question of when to stop the revoting procedure. There are two possible solutions: 1) If the number of lines to be detected is given, the program can be stopped when that number is accomplished, 2) If we know the feature differences between the expected lines and the unexpected ones, a threshold can be set according to the feature differences. In this study, we used the ratio of the number of feature points in the last and first detected lines to control the algorithm. This ratio was set to be 25% in this study. We found that the larger this ratio, the better the feature points map of the image could be and the less time the algorithm would consume. The adaptive selection criteria of this ratio should be further investigated in the future studies. This is particularly important for the real-time detection of pennation angles in the sonomyography technique, where the pattern of ultrasound images may change significantly during muscle contractions.

We also observed that there were several quite large values of the difference between the RVHT and the manual results. In those cases, it was noted that the detected lines represented image strips with relatively large widths. The current RVHT tended to locate the wide “line” along its edge, while the manual operation might more favor the skeleton of that “line”. Thus, when the direction of the central skeleton of a strip did not match that of its edges, a larger difference was generated between the angles detected by the two methods. In addition, among the 168 lines detected from the 45 ultrasounds images using RVHT, 3 lines did not correspond to any visibly identified lines in the image. According to our observation, the RVHT had counted together the edge/feature points belonging to different muscle fibers when the fiber image was quite blurred (subsequently the quality of the edge/feature points map was poor) or several short irrelative line segments happened to be collinear. SHT also has the similar defect, since detecting “broken line” in images is an inherent feature of the HT method. An HT method reported previously for the detection of broken lines (Song and Lyu 2005) could be integrated into the present method to solve this problem in the future.

Conclusion

In this paper we proposed a modified Hough transform using a revoting strategy, aiming at automatic estimation of the orientations of straight-line-shaped patterns in musculoskeletal ultrasound images. The method re-arranged the voting procedure of SHT to better locate the regional vote-leaders in the HT accumulator array under noisy situations. The results of both computer-generated images and clinical ultrasound images demonstrated that RVHT could provide an alternative approach for the orientation estimation for the lines in the ultrasound images. Further studies are required to achieve adaptive parameter selection for deciding the number of lines to be detected. Ultrasound image enhancement methods can also be used to make lines easier to be detected using the proposed method.

Acknowledgements

The authors would like to thank Mr. Qinghua Huang, Mr. Congzhi Wang, and Dr Micheal Ying for their help in data acquisition and analysis. The project was partially supported by the Research Grant Council of Hong Kong (PolyU 5245/03E) and The Hong Kong Polytechnic University (G-U064, G-YE22).

References

Ballard DH, Generalizing the Hough transform to detect arbitrary shapes, Pattern Recog., 1981; 13:111–122.

Bland JM, Altman DG, Statistical methods for assessing agreement between two methods of clinical measurement. Lancet 1986, 1:307-310.

Brown CM, Inherent bias and noise in the Hough transform, IEEE Trans. Pattern Anal. Machine Intell., 1983; 5:493- 505.

Duda RO, Hart PE, The use of Hough transform to detect lines and curves in pictures. Comm. Assoc. Comp. Machine, 1972; 15:11-15.

Fukunaga T, Ichinose Y, Ito M, Kawakami Y, Fukashiro S, Determination of fascicle length and pennation in a contracting human muscle in vivo. *J. Appl. Physiol. 1997;* 82:354-358.

Gonzalez R, Woods R, Digital Image Processing, Addison Wesley, 1992.

Guo JY, Zheng YP, Chan H, Huang QH, Chen X. Dynamic Monitoring of Forearm Muscles Using 1D Sonomyography (SMG) System. J. Rehabil. Res. Dev. Accepted. Jul 2007.

Hodges PW, Pengel LHM, Herbert RD, and Gandevia SC, Measurement of muscle contraction with ultrasound imaging. *Muscle Nerve 2003;* 27:682-692.

Hough PVC, Method and means for recognizing complex patterns, US patent 3069654, 1962.

Immerkær J, Some remarks on the straight line Hough transform. Pattern Recog. Lett., 1998; 19:1133–1135.

Ito M, Kawakami Y, Ichinose Y, Nonisometric behavior of fascicles during isometric contractions of a human muscle, *J. Appl. Physiol. 1998;* 85:1230-1235.

Itoii E, Sashi R, Minagawa H, Shimizu T, Wakavayashi I, Sato K, Position of immobilization after dislocation of the glenohumeral joint, J. Bone Joint Surg., 2001, 83A:661-667.

Kiryati N, Bruckstein AM, Antialiasing the Hough transform, CVGIP: Graphical Models and Image Processing, 1991; 53:213-222.

Kiryati N, Eldar Y, Bruckstein, A.M., A probabilistic Hough transform, Pattern Recog., 1991; 24:303-316.

Kiryati N, Lindenbaum M, Bruckstein AM, Digital or analog Hough transform?, Pattern Recog. Lett., 1991; 12:291-297.

Lam WCY, Lam LTS, Yuen KSY, Leung DNK, An analysis on quantizing the Hough space, Pattern Recog. Lett. 1994; 15:1127-1135.

Mademli L, Arampatzis A, Behaviour of the human gastrocnemius muscle architecture during submaximal isometric fatigue. *Euro. J. Appl. Physiol.* 2005; 94:611-617.

Maganaris CN, Baltzopoulos V, Sargeant AJ, Human calf muscle responses during repeated isometric plantarflexions. J. Biomechanics 2006; 39:1249-1255.

Maganaris CN, Baltzopoulos V, Sargeant AJ, Repeated contractions alter the geometry of human skeletal muscle. *J. Appl. Physiol. 2002;* 93:2089-2094.

Misuri G, Colagrande S, Gorini M, Iandelli I, Mancini M, Duranti R, and Scano G, In vivo ultrasound assessment of respiratory function of abdominal muscles in normal subjects. *Eur. Respir. J. 1997;* 10:2861-2867.

Narici MV, Binzoni T, Hiltbrand E, Fasel J, Terrier F, Cerretelli P, In vivo human gastrocnemius architecture with changing joint angle at rest and during graded isometric contraction. *J. Physiol. 1996;* 1:287-297.

Princen J, Illingworth J, Kittler J, A hierarchical approach to line extraction based on the Hough transform, Comput. Vision, Graph. Image Proc., 1990, 52:57-77.

Reeves ND, Maganaris CN, Narici MV, Ultrasonographic assessment of human skeletal muscle size. *Eur. J. Appl. Physiol*. 2004; 91:116-118.

Reeves ND, Narici MV, Maganaris CN, In vivo human muscle structure and function: adaptations to resistance training in old age, Exp. Physiol. 1994, 89:675-689.

Shi J, Zheng YP, Chen X, and Huang QH. Measurement of muscle fatigue with sonomyography: Dimensional change of muscles detected from ultrasound images. Med. Eng. Phys. 29:472-479, 2007a.

Shi J, Zheng YP, Huang QH, and Chen X. Relationships among continuous sonomyography, electromyography and torque generated by normal upper arm muscles during isometric contraction. IEEE Trans. Biomed. Eng. In print. May 2007b.

Song J, Lyu MR, A Hough transform based line recognition method utilizing both parameter space and image space, Pattern Recog., 2005, 38:539-552.

Van Veen TM, Groen FCA, Discretization errors in the Hough transform, Pattern Recog., 1981; 14:137-145.

Yuen SY, Ma CH, An investigation of the nature of parameterization for the Hough transform, Pattern Recog. 1997; 30(6):1009-1040.

Zheng YP, Chan MMF, Shi J, Chen X, Huang QH. Sonomyography: Monitoring morphological changes of forearm muscles in actions with the feasibility for the control of powered prosthesis. Med. Eng. Phy. 28:405-415, 2006

Fig. 1 The diagram of the procedures of the proposed revoting Hough transform.

Fig. 2 Line detection results of a computer-generated image, using SHT. (a) the original image (256x256), (b) the image after adding Gaussian noise with a mean of 64 (gray level) and a standard deviation of 16, (c) the edge map acquired using Sobel edge detector, (d) the accumulator array, (e) the line detection results when the SHT threshold is set to 70% of the global maximum, (f) the results obtained with a threshold of 50% of the global maximum, (g) the noisier image obtained by adding to original image a Gaussian white noise with a mean of 64 and a standard deviation of 32, (h) the edge map of (g), (i) the accumulator array of (g), and (j), (k) and (l) are the line detection results using SHT with the threshold set to 70%, 50%, 40% of the global maximum, respectively. In each accumulator array image, grey levels 0 and 255 represent its minimum and maximum values.

Fig. 3 Line detection results for the image of Fig.1(g) using RVHT. (a) the accumulator array, with the global maximum locations marked out, which correspond to the two directions of the same straight line, (b) the first detected line, (c) the updated edge map after the feature points corresponding to the 1st line were removed, (d) the new HT accumulator array, with the new global maximum locations marked out, (e) the second detected line, (f) the updated edge map, (g)-(r) were arranged in the same fashion. Totally 6 lines were detected. In each accumulator array image, grey levels 0 and 255 represent its minimum and maximum values.

Fig. 4 Angle estimation results of a typical musculoskeletal ultrasound image. (a) the original image, (b) the Sobel edge map, (c) the accumulator array, (d) and (e) the results using SHT with thresholds of 80% and 60% respectively, (f) lines detected using RVHT, totally 5 lines were detected and their angles (between the detected line and the vector pointing from the up-left to bottom-left corner of the image) were marked out. The removal width for RVHT was 12 pixels, and the ratio threshold of the feature points (counts by number of pixels in the edge map) of the last and first lines was set to be 25%.

Fig. 5 The correlation between the angle estimation results obtained using RVHT and those drawn manually. The x-axis represents the mean of manual results by two operators and the y-axis represents the RVHT results. R is the Pearson product moment correlation coefficient.

Fig. 6 Comparison of the results obtained using the RVHT and manual methods. *ap, aa1* and *aa2* represent the angle estimation results obtained by the RVHT method, operator 1 and operator 2, respectively. Mean and SD represent the mean value and standard deviation of the difference *ap* – (*aa1*+*aa2*)/2.

Fig. 1

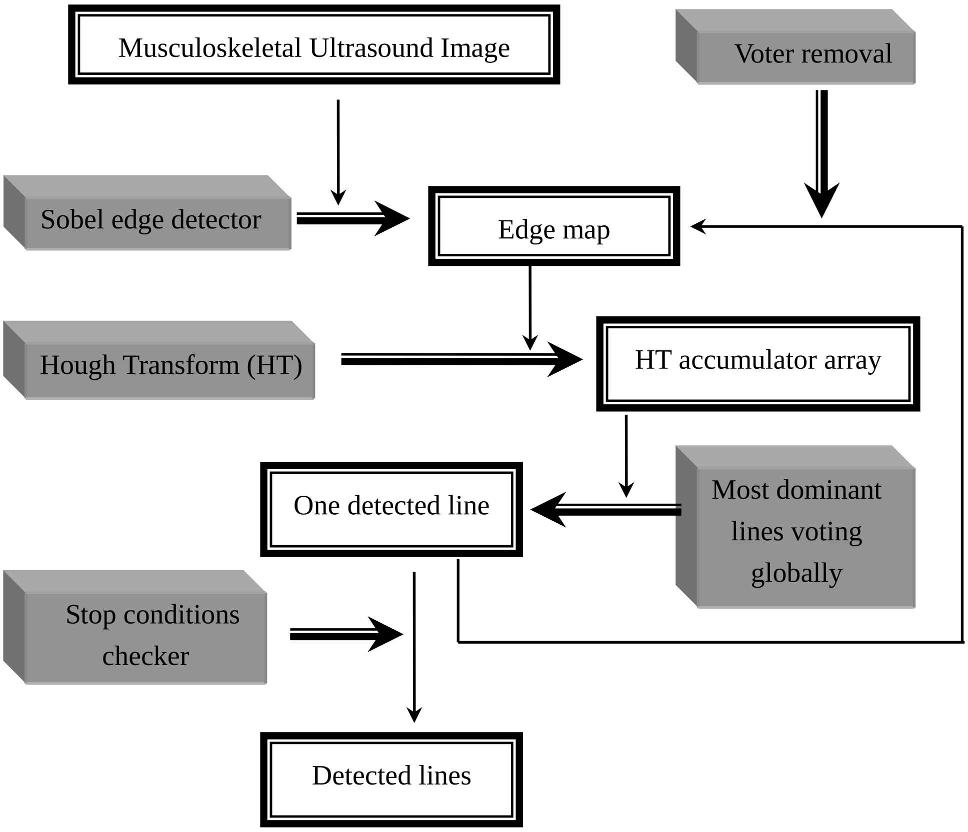
Musculoskeletal Ultrasound Image
Voter removal
Sobel edge detector
Edge map
Hough Transform (HT)
HT accumulator array
One detected line
Most dominant lines voting globally
Stop conditions checker
Detected lines

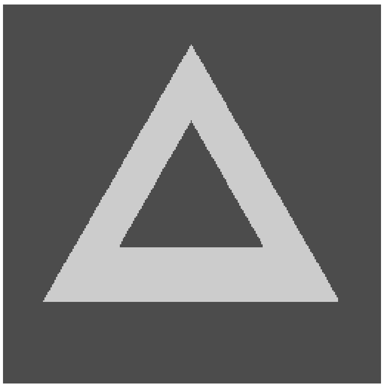

(a)

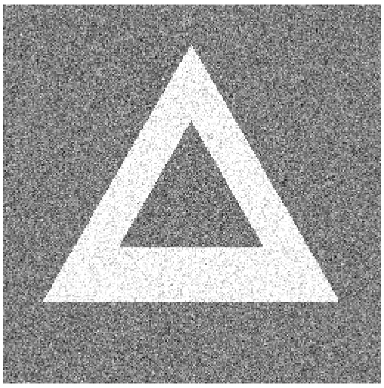

(b)

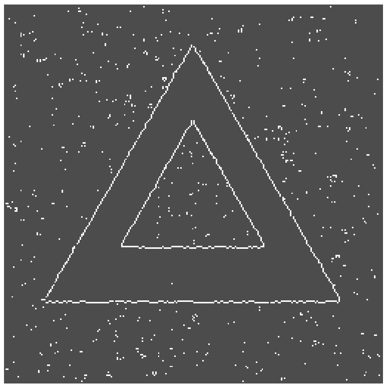

(c)

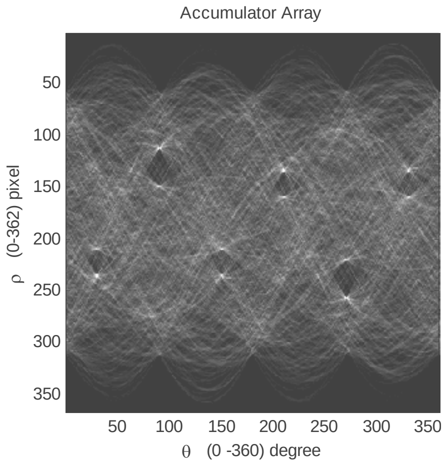

(d)

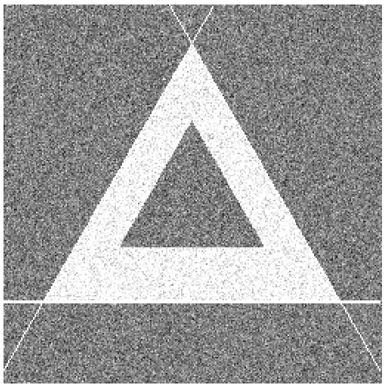

(e)

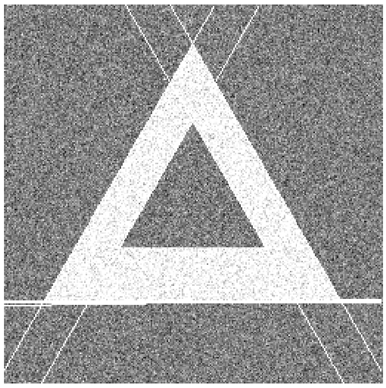

(f)

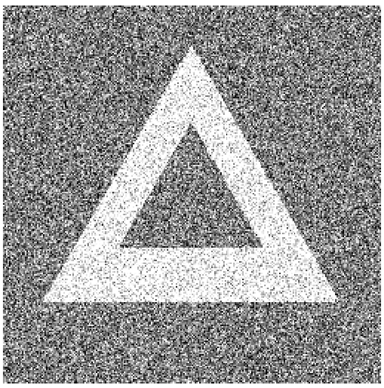

(g)

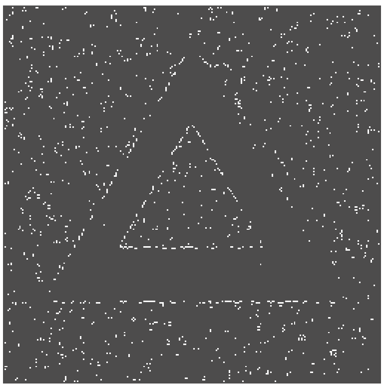

(h)

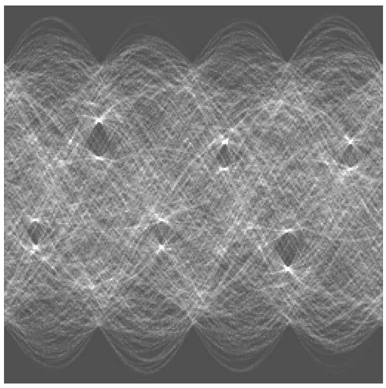

(i)

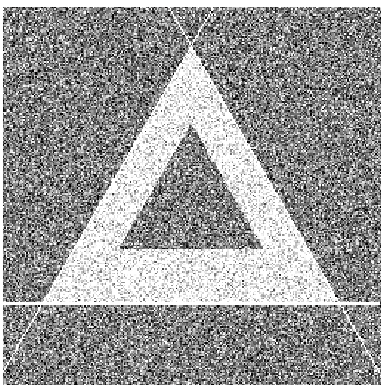

(j)

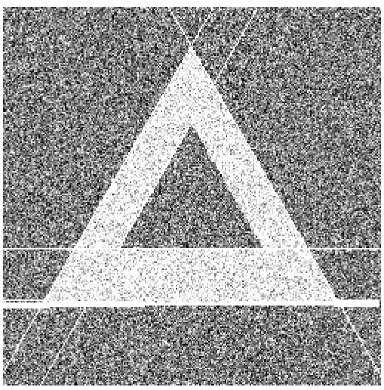

(k)

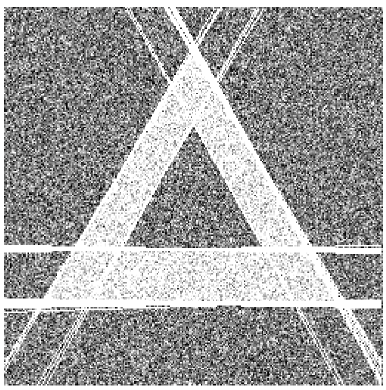

(l)

Fig. 3

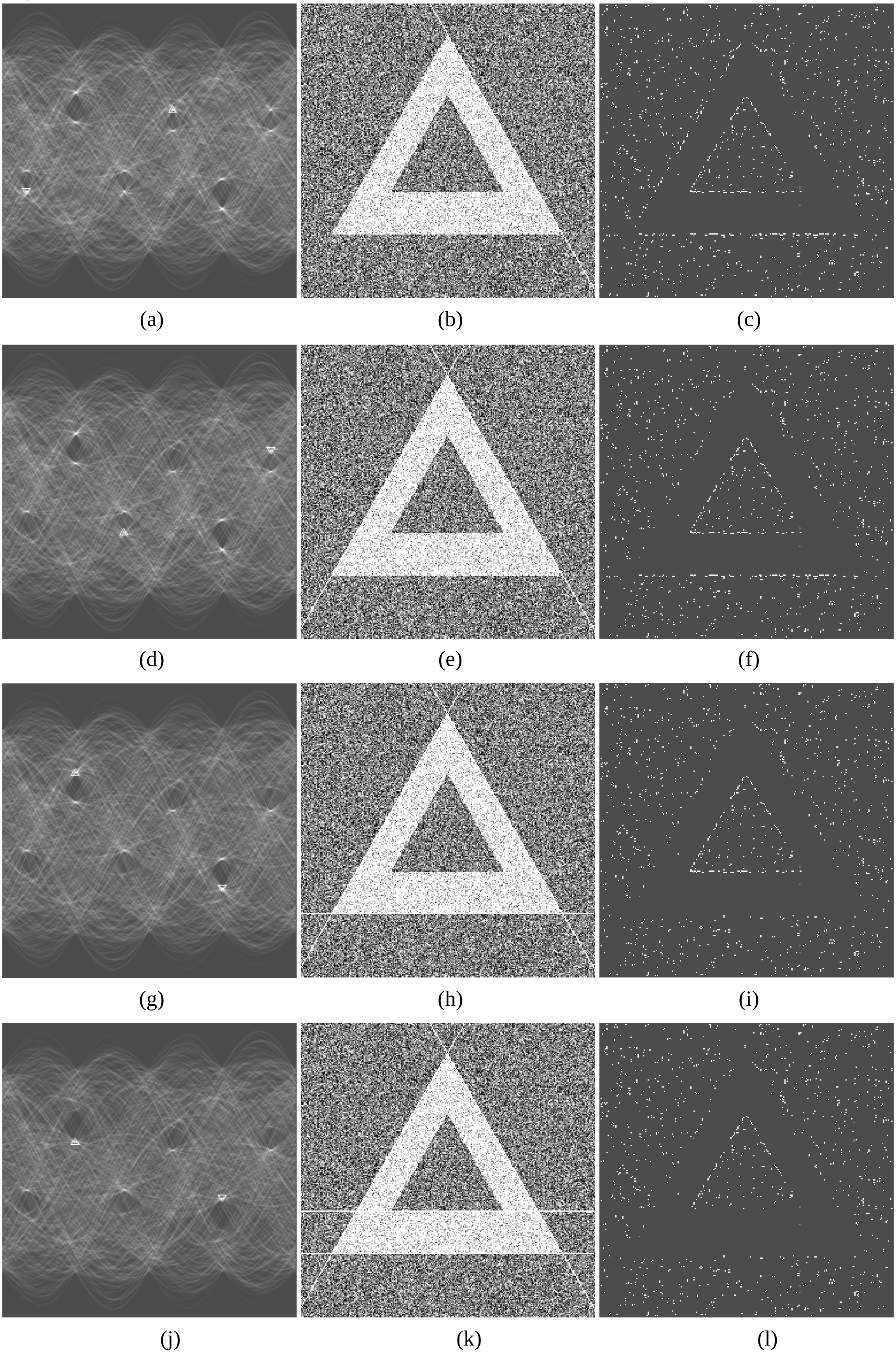

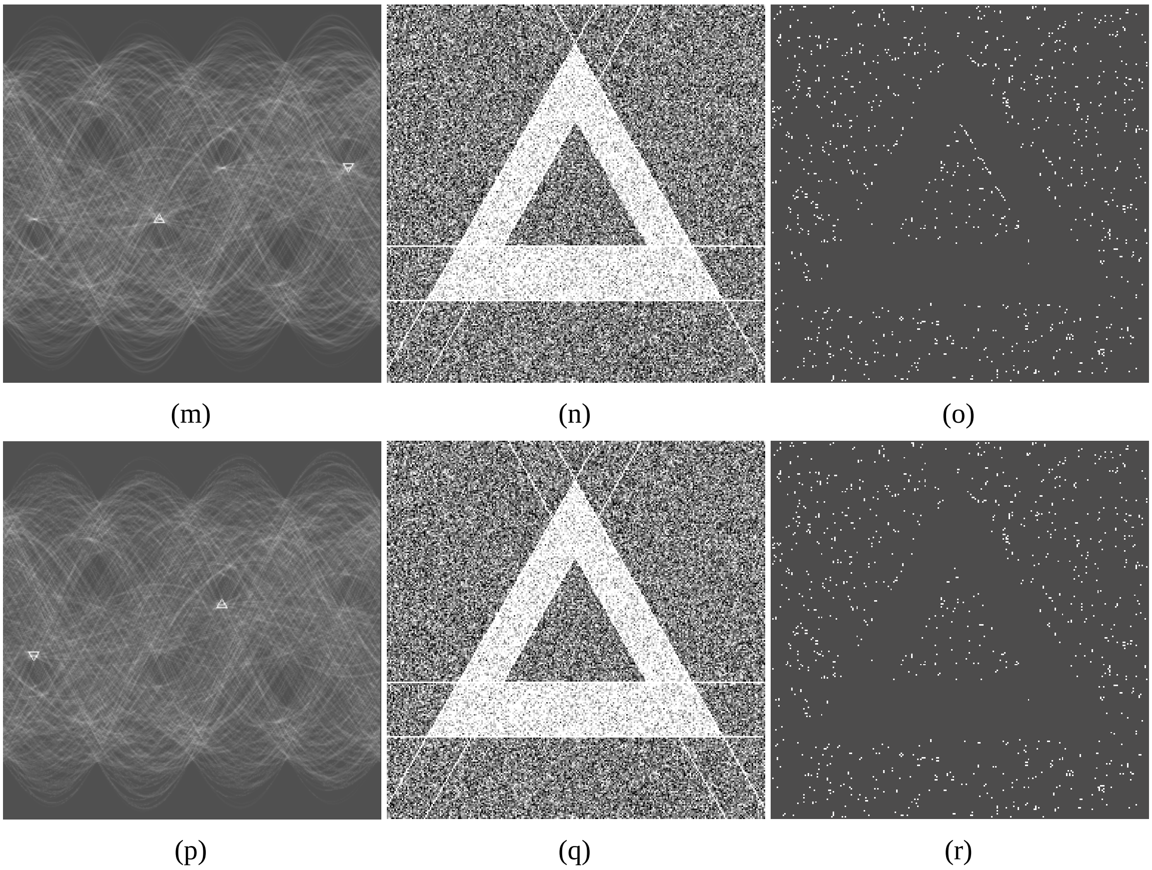

(m) (n) (o)

(p) (q) (r)

Fig. 4

(a)

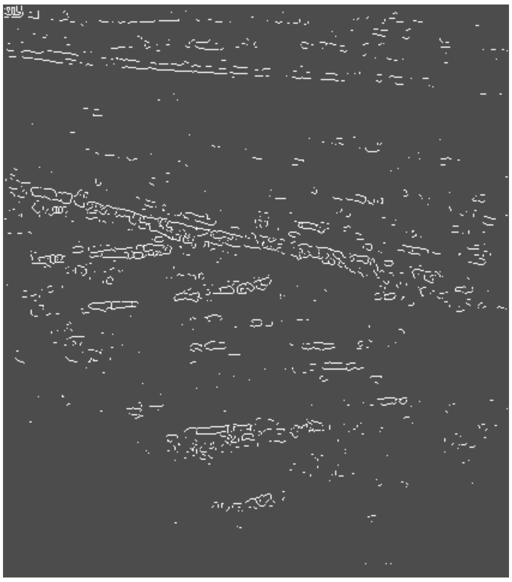

(b)

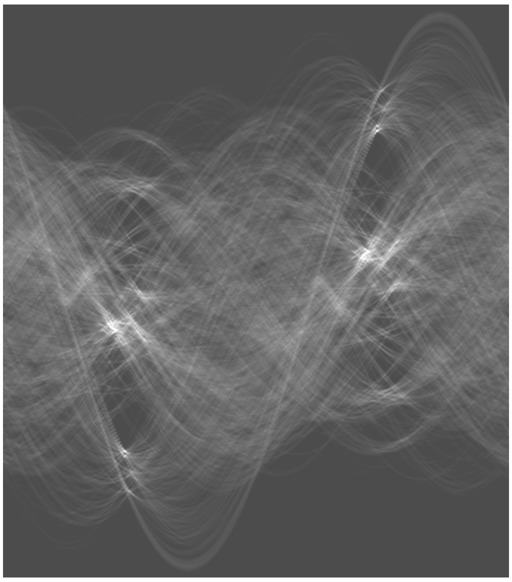

(c)

(d)

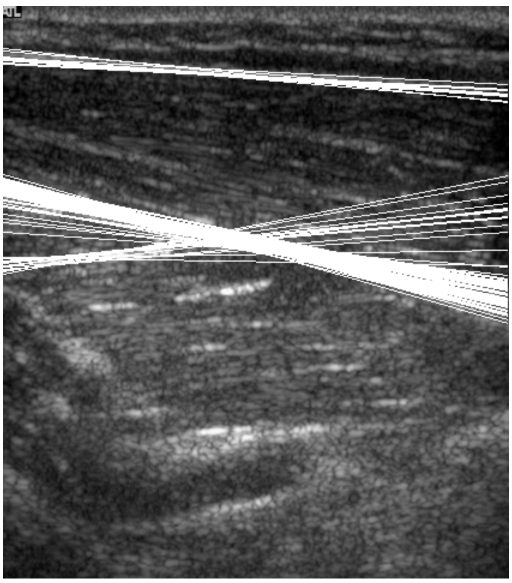

(e)

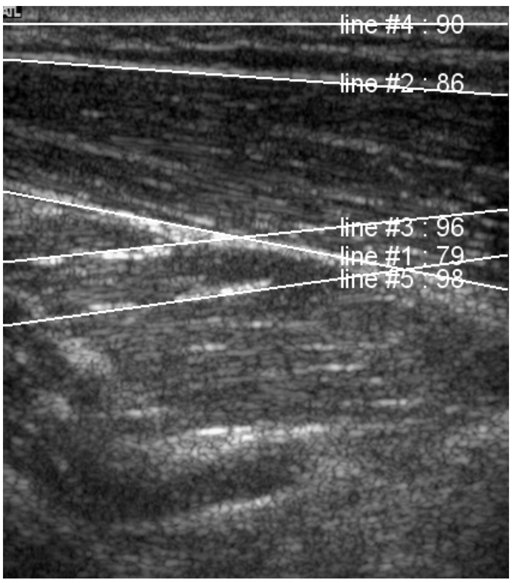

(f)

Fig. 5

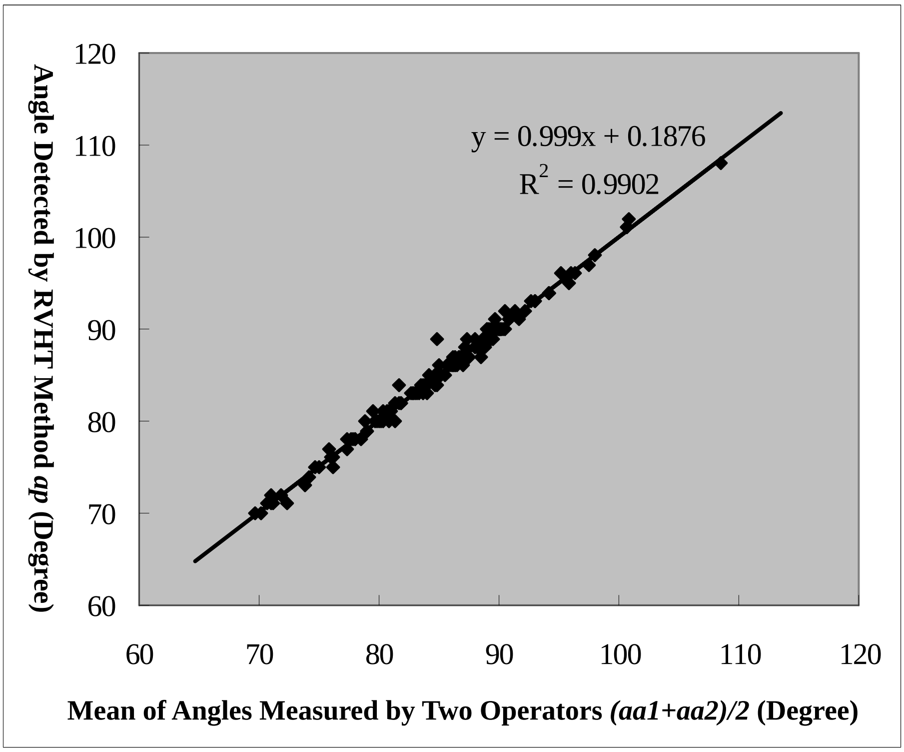

y = 0.999x + 0.1876
R^2 = 0.9902
120
110
100
90
80
70
60
60
70
80
90
100
110
120
Angle Detected by RVHT Method *ap* (Degree)
Mean of Angles Measured by Two Operators *(aa1+aa2)/2* (Degree)

Fig. 6

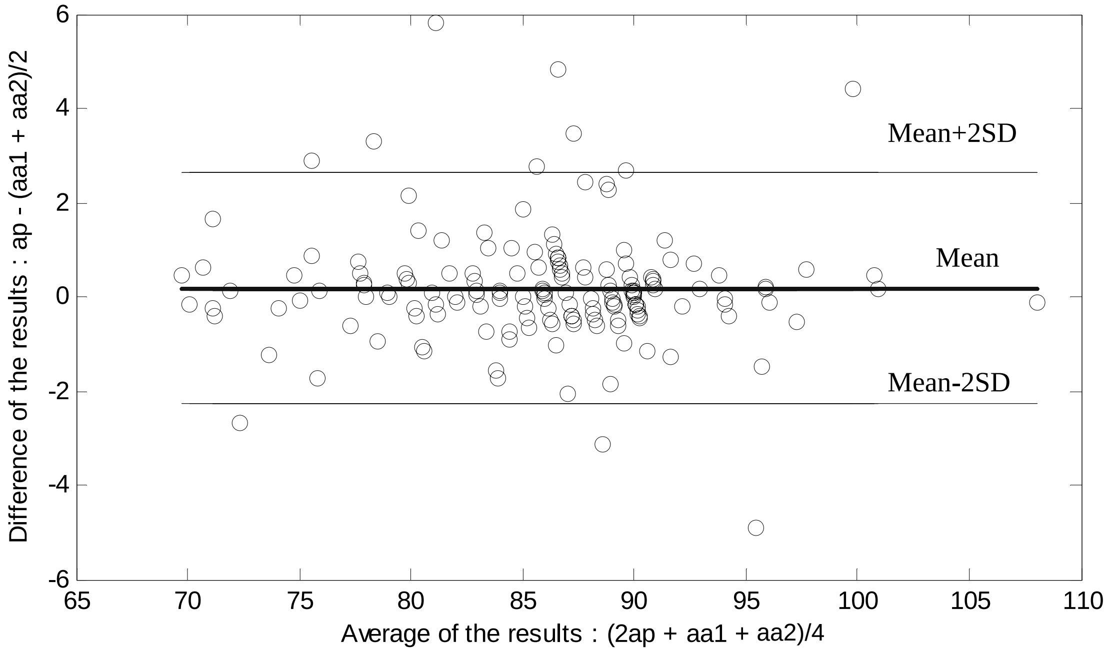
Mean+2SD
Mean
Mean-2SD
Difference of the results : ap - (aa1 + aa2)/2
Average of the results : (2ap + aa1 + aa2)/4
6
4
2
0
-2
-4
-6
65
70
75
80
85
90
95
100
105
110